# A Comparative Study of One-step and Stepwise Pyrolysis of Furfural Residue and its Kinetic Analysis

Liang Cheng, Yimeng Zhang, Jianbin Zhou,* and Shu Zhang *

Furfural residue (FR), a solid waste from the furfural production industry, is rich in cellulose and lignin. It has great potential for producing bio-fuels and bio-chemicals through pyrolysis. To examine the effects of heating programs on the product distribution of FR pyrolysis, stepwise and one-step pyrolysis processes were compared using a commercial Py-GC/MS system. During the stepwise pyrolysis, the acids had a maximum yield at 300 °C, while the outputs of the ketones/aldehydes, furans, esters, alcohols, and sugars were the most abundant at 350 °C. The production of aromatics increased, whereas the nitrogen-containing compounds decreased as the temperature increased from 300 °C to 500 °C. The relative percentages of the aromatics and furans from the one-step pyrolysis were much higher than those from the stepwise pyrolysis. In contrast, the acids, sugars, alcohols, nitrogen-containing compounds, and alkanes/olefins from the stepwise pyrolysis were higher than those from the one-step pyrolysis at 500 °C. The kinetic analysis showed that the activation energy of the FR was reduced from between 212 and 214 kJ/mol to between 189 and 191 kJ/mol as the degree of conversion ($\alpha$) increased from 20% to 60%, before increasing from 191 kJ/mol to 478 kJ/mol as $\alpha$ further increased from 70% to 90%.

*Keywords: Pyrolysis; Py-GC/MS; Furfural residue; Activation energy; Kinetics*

*Contact information: Department of New Energy Science and Technology, Nanjing Forestry University, Nanjing, Jiangsu 210037, P.R. China. *Corresponding author: zhoujianbin@njfu.edu.cn; zhangshuwo@hotmail.com or s.zhang@njfu.edu.cn*

## INTRODUCTION

Furfural residue (FR) is the solid byproduct generated from the furfural production process, where the hemicellulose in biomass is catalytically hydrolyzed by a diluted acid, usually $H_2SO_4$. The total global furfural production is approximately 0.25 million metric tons (mmt)/yr, of which approximately 70% is produced in China (Zeitsch 2000; Rong 2012), mostly using corn cob as the raw material (Cui 2014). The majority of FR (approximately 2.4 mmt/yr to 3.0 mmt/yr) in China is simply stored as post-process biomass waste without being further utilized (Yin *et al*. 2011). As FR contains acidic functional groups, inorganic minerals, and some organic volatile compounds, the simple storage of FR is not only a waste of land and valuable material, but also has a negative environmental impact (Yin *et al*. 2011). Thus, the proper treatment of FR is a realistic solution to ensure that the development of the furfural industry is both environmentally friendly and socio-economically sustainable.

As FR is rich in cellulose (43.9%) and lignin (45.1%) (Sun 2011) and features a higher heating value of 20.87 MJ/kg (Cheng *et al.* 2017), it can ideally be recycled as a green resource for bioenergy production. Previous research (Zheng *et al*. 2016) has tried to use FR to produce bioethanol, but the components of lignin can reduce the accessibility of cellulose to enzymes and decrease the hydrolysis rate of cellulose (Eriksson *et al*. 2002; Alvira *et al*. 2010). A proper pretreatment with alkaline peroxide/salts has proven effective at removing lignin from FR for bioethanol production (Xing *et al*. 2012; Yu *et al*. 2015). However, the extraction of lignin with waste salt water can still be problematic in the long term.

A thermochemical process can efficiently convert biomass to different biochemical products under a variety of conditions. Besides direct combustion for heat production, the simultaneous production of bio-gas and bio-carbon can be achieved by a gasification process in an $O_2$-deficient reaction atmosphere (Cheng *et al.* 2017). As a simple and effective process, the pyrolysis (with no $O_2$) of biomass can produce liquid bio-fuels (bio-oil) and highly valuable bio-chemicals. Indeed, pyrolysis is considered to be the initial step for all thermal conversion processes. The high lignin content in FR means a high output of aromatic chemicals, which are the active ingredients in pesticides, adhesives, and other bio-chemical products. Thus, pyrolysis is likely an economical option for the utilization of FR, which has been rarely studied so far.

The temperature and heating rate are the key parameters that affect the product yields and components of pyrolysis. To maximize the liquid products, the biomass pyrolysis in the literature is usually set to the temperature range of 450 °C to 550 °C (Azeez *et al*. 2010; Lv and Wu 2012; Cheng *et al*. 2015a). This wide temperature range implies that the pyrolysis behavior of each biomass is individual; hence, the optimal pyrolysis conditions for FR need to be investigated separately. Also, during industrial production, the reaction scale is much larger, whereas the temperature increasing process is relatively moderate. Because of the difference in the heating rate, the pyrolysis outputs from industrial productions can be vastly different from those from one-step pyrolysis in an analytical instrument, such as a pyrolysis-gas chromatograph/mass spectrometer (Py-GC/MS). Indeed, the stepwise process as a simple approach can probe the effect of heat transferring rates by intermittently holding the temperatures at different stages.

Pyrolysis process involves a series of chemical reactions from which both the resultant products and the reaction kinetics (*e.g.* activation energy) are important parameters when considering the applicability. The furfural residue and its resultant char are literally mixtures (without definite molecular structures), rather than being pure materials or chemical compounds. Such a situation leads to complexity in its kinetic behavior during the pyrolysis reactions. Thus, a detailed kinetic study of FR is necessary for its further study and utilization.

In this study, the pyrolysis behaviors of FR under one-step and stepwise temperature increasing conditions were both analyzed and compared using an integrated Py-GC/MS system. Furthermore, the kinetics of FR pyrolysis were studied with a thermogravimetric (TG) analyzer.

## EXPERIMENTAL

### Materials

The FR was obtained from a furfural production plant in Hebei Province, China, which used corn cob as the raw material (Lu 2005). Following pulverization, particles between 150 µm and 250 µm were selected for the experiments. The basic chemical properties of the FR were analyzed and are shown in Table 1.

## Methods

### *Pyrolysis experiments*

The pyrolysis processes were performed on a CDS Pyroprobe 5000 Series pyrolyzer (CDS Analytical, Oxford, PA, USA), coupled with a Clarus 680 GC (PerkinElmer, Waltham, USA) and a Clarus SQ 8 T MS (PerkinElmer). For each test, approximately 0.5 mg sample was loaded into a quartz tube, and both sides of the tube were blocked with quartz wool. The quartz tube with the sample was then placed into the pyroprobe and heated from 50 °C to the target temperature at a heating rate of 20 °C/ms with 15 s of holding time at the target temperature. For the one-step pyrolysis of the FR, the target temperature was set at 500 °C; for the stepwise pyrolysis, one sample was used for the whole series of tests at the temperatures of 300 °C, 350 °C, 400 °C, and 500 °C, which were carried out in sequence. The corresponding chromatograms and mass spectra at each pyrolysis temperature were acquired. Figure 1 shows the flowchart of the stepwise pyrolysis of the FR.

**Table 1.** Basic Chemical Properties of the FR

| | |
|---|---|
| Moisture (wt.%) | 5.56 |
| Ash (wt.%) | 8.99 |
| Volatile Compounds (wt.%) | 64.74 |
| Fixed Carbon (wt.%) | 26.27 |
| C (wt.%) | 53.52 |
| H (wt.%) | 1.67 |
| N (wt.%) | 0.63 |
| S (wt.%) | 0.78 |
| O (wt.%) | 34.42 |
| Na (wt.%) | 0.30 |
| K (wt.%) | 3.36 |
| Ca (wt.%) | 0.35 |
| Mg (wt.%) | 0.22 |
| Al (wt.%) | 0.43 |
| Cellulose (wt.%) | 37.95 |
| Hemicellulose (wt.%) | 2.29 |
| Lignin (wt.%) | 42.04 |
| Organic solubles (wt.%) | 8.73 |
| All of the data, except for the moisture content, were on the dry basis. | |

The pyrolysis vapor was transferred into the GC column through a transfer line maintained at 280 °C, and then separated by an Elite-5MS capillary column (30 m × 0.25 mm, 0.25 μm film thickness) (PerkinElmer). The inlet temperature was held at 40 °C for 2 min, and then increased to 295 °C at 8 °C/min with a holding time of 5.5 min. The carrier gas was helium (99.999%) with a flow rate of 1 mL/min, and the split ratio was 1:50. The MS was operated in the EI+ mode, and the collected mass spectra were in the range of 35 m/z to 550 m/z.

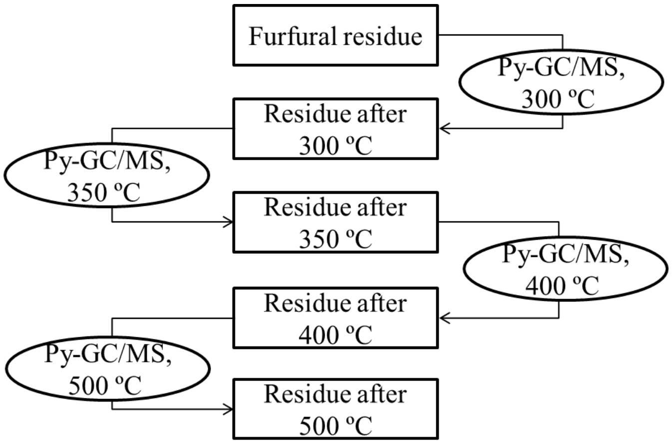

**Fig. 1.** Flowchart of the stepwise temperature increase during the pyrolysis of the FR

*Kinetic analysis*

The kinetic study experiments were conducted on a PerkinElmer STA 8000 Simultaneous Thermal Analyzer. An approximately 10 mg sample was loaded into the crucible for each test. It was then heated from 50 °C to 750 °C at the different heating rates of 10 °C/min, 20 °C/min, 30 °C/min, and 50 °C/min, while helium constantly flowed through the reaction zone as the carrier gas at a rate of 50 mL/min. The kinetic methods of Coats-Redfern (CR) (Coats and Redfern 1964; Liu 2011; Jiang *et al*. 2012) and Flynn-Wall-Ozawa (FWO) (Opfermann and Kaisersberger 1992; Liu 2011; Jiang *et al*. 2012; Slopiecka *et al*. 2012) were used to calculate the activation energy ($E_\alpha$) values. The Arrhenius plot of the CR method was $\ln(\beta/T^2)$ against $1/T$, and the slope was $-E_\alpha/R$. The Arrhenius plot of the FWO method was $\ln\beta$ against $1/T$, and the slope was $-1.052E_\alpha/R$. The $E_\alpha$ values could be therefore calculated from the slope of the plots,

$$\text{CR method: } \ln[\beta/(T^2(1-2RT/E_\alpha))] = \ln[AR/(E_\alpha G(\alpha))] - E_\alpha/RT \tag{1}$$

$$\text{FWO method: } \ln\beta = \ln[(AE_\alpha)/(RG(\alpha))] - 5.331 - 1.052E_\alpha/RT \tag{2}$$

where $\alpha$ is the conversion rate (%), $\beta$ is the heating rate (K/min), $R$ is the universal gas constant (8.314J/(mol • K)), $T$ is the temperature (K), $A$ is the pre-exponential factor, and $G(\alpha)$ is the kinetic mechanism function.

## RESULTS AND DISCUSSION

### One-step Pyrolysis

The one-step pyrolysis of the FR was performed at 500 °C. The main 30 compounds were identified by GC/MS and are listed in Table 2. According to the different functionalities of the molecules, these main compounds were classified into nine groups, which were acids, ketones/aldehydes, aromatics, furans, esters, sugars, alcohols, nitrogen-containing compounds, and alkanes/olefins. Their relative contents (area% obtained from the chromatograms) are presented in Fig. 2. Generally, the most abundant outputs were aromatics and furans (relative contents > 20%), whereas the alcohol and nitrogen-containing compound contents were nearly negligible. Meanwhile, the amounts of acids (mainly acetic acid), ketones/aldehydes, esters, sugars, and alkanes/olefins were moderate.

**Table 2.** Relative Contents of the Chemical Compounds in Different Functional Groups from the Two Different Pyrolysis Processes of the FR in the Py-GC/MS

| Chemical | | One-step Pyrolysis at 500 °C | Stepwise Pyrolysis | | | |
|---|---|---|---|---|---|---|
| | | | 300 °C | 350 °C | 400 °C | 500 °C |
| | Acetic acid | 2.42 | - | - | - | - |
| Acids (%) | n-Hexadecanoic acid | 1.57 | 2.58 | 0.24 | - | - |
| | Pentanoic acid, 4-oxo- | - | 3.05 | - | - | - |
| | Octadecanoic acid | - | 0.61 | 0.49 | - | - |
| | Oleic Acid | 0.75 | 0.46 | - | - | - |
| | 9,12-Octadecadienoic acid (Z,Z)- | - | 0.28 | - | - | - |
| | Tetradecanoic acid | - | 0.34 | - | - | - |
| | Pentadecanoic acid | - | 0.29 | - | - | - |
| | Palmitoleic acid | - | 0.35 | - | - | - |
| | Dodecanoic acid | - | 0.22 | - | - | - |
| | Z-3-Methyl-2-hexenoic acid | - | - | - | 0.19 | - |
| Ketones/Aldehydes (%) | 5,8-Decadien-2-one, 5,9-dimethyl-, (E)- | - | 0.10 | - | - | - |
| | 1,2-Cyclopentanedione | 1.48 | - | - | - | - |
| | Benzyl methyl ketone | 1.23 | - | - | - | - |
| | 2-Propanone, 1-(acetyloxy)- | - | - | - | - | - |
| | 4H-Pyran-4-one, 2,3-dihydro-3,5-dihydroxy-6-methyl- | - | 0.11 | - | - | - |
| | 2-Cyclopenten-1-one, 2-hydroxy- | - | - | 0.63 | 0.54 | - |
| | 2-Propanone, 1-hydroxy- | 1.40 | - | 1.04 | 0.66 | - |
| | 1,2-Cyclopentanedione, 3-methyl- | 0.91 | 0.17 | 0.18 | 0.28 | - |
| | Succindialdehyde | - | - | 0.21 | 0.23 | - |
| Aromatics (%) | Phenol | 2.82 | 0.10 | 0.22 | 0.43 | 0.82 |
| | 2-Methoxy-4-vinylphenol | 4.92 | 0.53 | 1.05 | 0.58 | 0.14 |
| | Phenol, 2-methoxy- | 3.03 | - | 0.32 | 0.51 | 0.25 |
| | Phenol, 2,6-dimethoxy- | 1.20 | - | 0.18 | 0.31 | 0.12 |
| | Phenol, 4-ethyl-2-methoxy- | 0.9 | - | - | 0.23 | 0.11 |
| | Phenol, 4-ethyl- | 1.41 | - | - | 0.23 | 0.29 |
| | p-Cresol | 1.65 | - | - | 0.31 | 0.65 |
| | Toluene | - | - | - | - | 0.17 |
| | Phenol, 3-ethoxy- | - | - | - | - | 0.65 |
| | Phenol, 3-ethyl-5-methyl- | - | - | - | - | 0.15 |
| | Phenol, 2,4-dimethyl- | - | - | - | - | 0.12 |
| | 4-Ethylcatechol | - | - | - | - | 0.14 |
| | Benzenemethanol, 3-hydroxy-5-methoxy- | - | - | - | - | 0.10 |
| | Benzene, 1-methoxy-4-methyl- | - | - | - | - | 0.10 |
| | 3-Methoxy-5-methylphenol | - | - | - | - | 0.07 |

| | | | | | | |
|---|---|---|---|---|---|---|
| | Styrene | - | - | - | - | 0.08 |
| | 1,2-Benzenediol, 4-methyl- | - | - | - | - | 0.41 |
| | 1,2-Benzenediol, 3-methyl- | 0.84 | - | - | - | - |
| | p-Xylene | - | - | - | - | 0.07 |
| | 1,2-Benzenediol, 4-methyl- | - | - | - | - | 0.27 |
| | Phenol, 2-methyl- | - | - | - | - | 0.23 |
| | Vanillin | 0.85 | 0.31 | - | - | - |
| | Catechol | 1.69 | - | 0.19 | - | - |
| | 1,2,4-Trimethoxybenzene | - | - | - | 0.23 | - |
| | 1,3-Benzenediol, 4-ethyl- | - | - | - | 0.18 | - |
| | Creosol | 2.84 | - | - | 0.65 | - |
| | 1,2-Benzenediol, 3-methoxy- | 1.98 | - | - | 0.35 | - |
| | Phenol, 4-methoxy-3-(methoxymethyl)- | 0.78 | - | - | - | - |
| | 3-tert-Butyl-4-hydroxyanisole | 0.76 | - | - | - | - |
| Furans (%) | 5-Hydroxymethylfurfural | 8.18 | 1.18 | 0.77 | 0.31 | - |
| | Benzofuran, 2,3-dihydro- | 6.68 | 1.01 | 2.37 | 1.31 | 0.29 |
| | Furfural | 2.42 | 0.44 | 0.46 | 0.33 | 0.11 |
| | 2-Furancarboxaldehyde, 5-methyl- | 1.02 | 0.17 | 0.28 | - | - |
| | 2,5-Furandione, 3-methyl- | - | 0.13 | - | - | - |
| | 2(5H)-Furanone | 1.04 | - | 0.34 | 0.22 | |
| | Furan, 2,5-dimethyl- | - | - | 0.15 | - | 0.12 |
| | 2,5-Dimethyl-4-hydroxy-3(2H)-furanone | - | - | 0.21 | - | - |
| | 2-Furanmethanol | 0.77 | - | 0.83 | - | - |
| | Methyl methacrylate | - | - | - | 0.53 | 0.52 |
| | Furan, 2-methyl- | - | - | - | 0.55 | 0.26 |
| | 2-Cyclopenten-1-one, 3-methyl- | - | - | - | - | 0.09 |
| Esters (%) | 3-Furancarboxylic acid, methyl ester | - | 0.20 | - | - | - |
| | Propanoic acid, 2-oxo-, methyl ester | 1.04 | - | 0.48 | 0.35 | - |
| | Acetic acid, 2-ethylbutyl ester | - | - | 0.25 | 0.35 | - |
| | Acetic acid, 4-methoxy-2-(3-methyl-6-oxo-hex-2-enyl)-phenyl ester | - | - | - | - | 0.09 |
| | Methyl methacrylate | 1.19 | - | - | - | - |
| Sugars (%) | Levoglucosan | 1.75 | 1.25 | 1.19 | 1.44 | 1.56 |
| | α-D-Glucopyranoside, O-α-D-glucopyranosyl-(1.fwdarw.3)-β-D-fructofuranosyl | - | 0.13 | - | - | - |
| | Maltol | - | - | 0.44 | 0.18 | - |
| Alcohols (%) | Glycerin | - | 0.44 | - | - | - |
| | Ethanol, 2-(2-butoxyethoxy)- | - | 0.18 | - | - | - |
| | Cyclopropyl carbinol | - | - | 0.65 | 0.28 | - |
| | 2-Pentanol, 5-(2-propynyloxy)- | - | - | 0.59 | 0.39 | - |

| | | | | | | |
|---|---|---|---|---|---|---|
| Nitrogen-containing compounds (%) | 3-Pyridinol | - | 0.93 | - | - | - |
| | 3-Diethylamino-2,2-dimethylpropionaldehyde | - | 0.4 | - | - | - |
| | Pyrrolidine, 2-butyl-1-methyl- | - | - | 0.23 | - | - |
| | Pyridine, 3-methoxy- | - | - | 0.19 | - | - |
| | N-Butyl-tert-butylamine | - | - | 0.00 | - | - |
| | 4(1H)-Pyrimidinone, 6-methyl- | - | - | 0.15 | 0.21 | - |
| Alkanes/ Olefins (%) | 1-Methoxyadamantane | - | 0.15 | - | - | - |
| | Squalene | - | 0.54 | 0.24 | 0.15 | - |
| | Limonene | - | - | 0.25 | 0.96 | 0.32 |
| | 2-Carene | - | - | - | - | 0.07 |

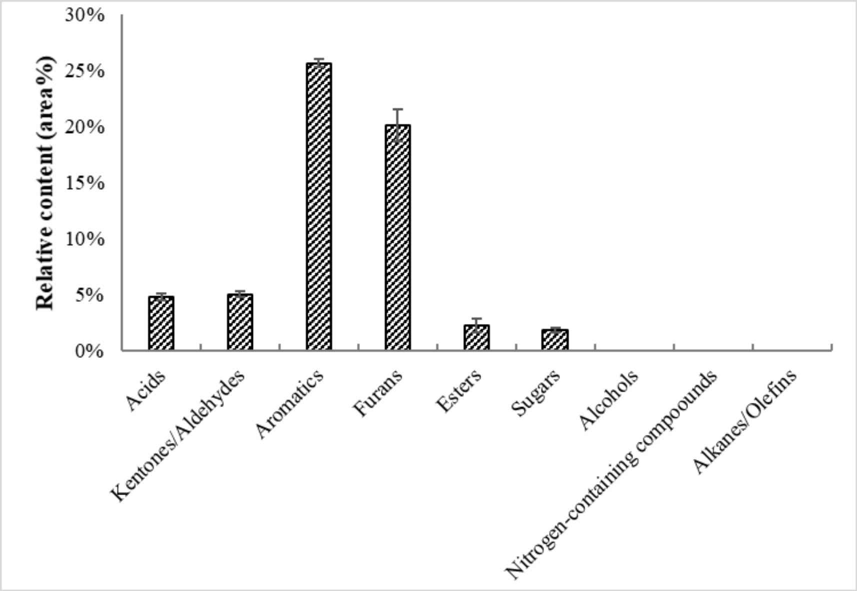

**Fig. 2.** Distribution of the chemical compounds from the one-step pyrolysis of the FR at 500 °C

Cellulose, hemicellulose, and lignin are all sources for pyrolytic acetic acids, mainly from acetyl groups (Demirbaş 2000). Because most acetyl groups are attached to pentosans and split off during the hydrolysis processing of the corn cob for furfural production, it was reasonable to observe that the acids output from the FR was not high. Hemicellulose is the major contributor for the generation of ketones (Lv and Wu 2012). After the furfural production process, the content ratio of hemicellulose to cellulose in the materials decreases greatly from 1.475 to 0.082 (Sun 2011). Therefore, a lower ketone output from the FR pyrolysis was observed. Aromatics is a general name for benzene ring-containing chemicals (mostly phenolic components), which are mainly derivatives of lignin. Therefore, the aromatic content from the FR was the highest. Additionally, benzofuran, 2,3-dihydro- was classified in the furans group. According to the report by Lu (2010), a large amount of benzofuran, 2,3-dihydro- was also detected in the pyrolysis products from bagasse lignin, but a low amount was detected in the products from timber lignin, which was mainly because of the difference in the lignin structure. Furans were the second key group from the one-step FR pyrolysis, mainly because of the decomposition of cellulose (Lv and Wu 2012). Additionally, the alkali and alkaline earth metallic (AAEM) elements in the FR may have played a role in promoting the conversion of sugars into furans (Patwardhan *et al*. 2010; Mourant *et al*. 2011; Cheng *et al*. 2015a).

## Stepwise Pyrolysis

Stepwise pyrolysis with a Py-GC/MS is a simple method that can reflect the effects of the heating program on the yield and distribution of the products. Chemical outputs from the stepwise pyrolysis of the FR at 300 °C, 350 °C, 400 °C, and 500 °C were identified and classified in the same manner mentioned above and are listed in Table 2 for easy comparison. The chemical distribution of the pyrolysis outputs of the FR by stepwise pyrolysis is presented as their relative contents (area%) in Fig. 3, where the sum of the peak areas of the whole four-stage test at different temperatures (300 °C, 350 °C, 400 °C, and 500 °C) was taken as the total area (100%) for a sample.

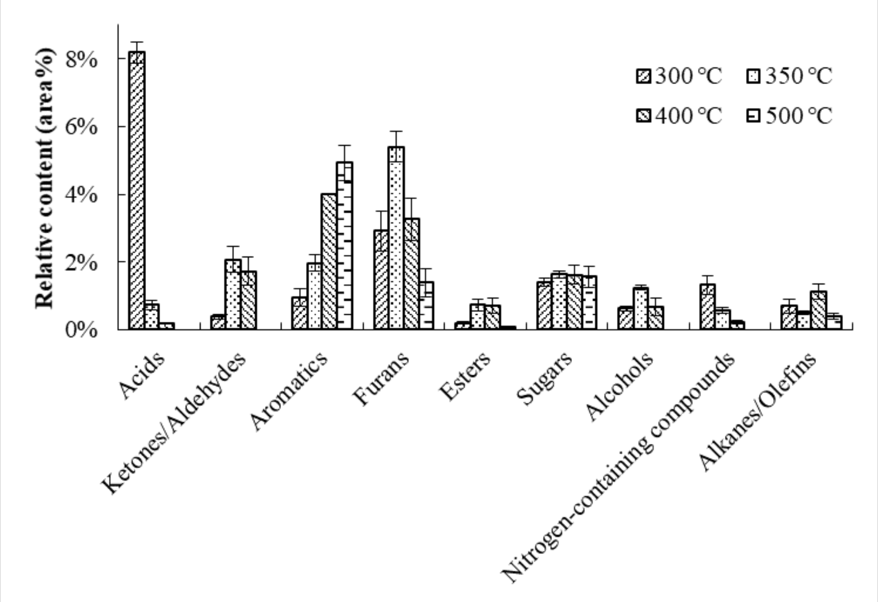

**Fig. 3.** Distribution of the chemical compounds from the stepwise pyrolysis of the FR at 300 °C, 350 °C, 400 °C, and 500 °C

Apparently, of all the chemical groups, the acids had the highest relative content (8.19%) at 300 °C, but they decreased dramatically to only 0.72% as the temperature increased to 350 °C. When the temperature further increased to 500 °C, there were nearly no acids identified. At 300 °C, the decomposition of cellulose and lignin are both very limited. Thus, the low temperature of 300 °C could only yield a relatively low degree of decomposition. The acids generated at this temperature mostly featured large molecular weights (pentanoic acid, 4-oxo- and n-hexadecanoic acid, *etc.*), rather than being acetic acids.

The ketones/aldehydes group was relatively abundant at 350 °C (2.07%) and 400 °C (1.72%) compared with 300 °C (0.38%), and few ketones/aldehydes were detected at 500 °C. Because lignin has no contribution to the generation of ketones/aldehydes (Lv and Wu 2012), the ketones/aldehydes must have been from the cellulose in the FR. The decomposition of cellulose is intensive between 315 °C to 400 °C, which is higher compared with 220 °C to 315 °C for hemicellulose decomposition (Yang *et al*. 2007). Therefore, ketones/aldehydes were not observed at 500 °C. The minor amount of ketones/aldehydes detected at 300 °C could have been derived from the remaining hemicellulose in the FR after the hydrolysis of the corn cob.

The output of aromatics continuously increased as the temperature increased, from 0.94% at 300 °C to 4.92% at 500 °C. The precursor for aromatics in biomass is mainly lignin (Lv and Wu 2012). Meanwhile, the number of aromatic species also increased from 2 to 20 as the temperature increased from 300 °C to 500 °C, which indicated a complex and refractory lignin structure.

The output of furans increased from 2.92% (300 °C) to 5.40% (350 °C), and then decreased to 1.39% (500 °C). As cellulose has a maximum decomposition rate at approximately 350 °C (Yang *et al*. 2007), the formation of furans was largely attributed to the decomposition of cellulose. The number of furan species at different temperatures did not change considerably (5 for 300 °C, 8 for 350 °C, 6 for 400 °C, and 6 for 500 ºC) compared with the change in the aromatics species because of the stable basic structural units of cellulose. Meanwhile, Figs. 2 and 3 indicate that the FR had a higher output of furans than ketones/aldehydes during both pyrolysis modes.

The sugars in the outputs of the FR were mostly levoglucosan, which was the primary unit of the cellulose decomposition, while all of the other chemical outputs from cellulose could be considered the secondary decomposition of levoglucosan. The output of sugars was higher at 350 °C (1.63%) and 400 °C (1.62%), but lower at 300 °C (1.39%) and 500 °C (1.56%). However, these differences were fairly minor.

A massive reduction in the nitrogen-containing compounds was found as the temperature increased from 300 °C to 500 °C, whereas there were almost no nitrogen-containing compounds detected during the one-step pyrolysis. This indicated that lower pyrolysis temperatures could retain nitrogen in the organic products, whereas higher pyrolysis temperatures in the one-step pyrolysis could promote the formation of gaseous $NO_x$. Esters and alcohols both had their highest output at 350 °C, which implied a close relationship with the decomposition of cellulose. The changing trend of the alkanes/olefins remained unclear.

The relative percentages of the identified output chemicals from the one-step and stepwise pyrolysis of the FR are compared in Fig. 4. Clearly, the aromatics group had a remarkably higher relative percentage in the one-step pyrolysis (43.10%) than in the stepwise pyrolysis (22.21%). Because the decomposition of lignin and the generation of aromatic components need a relatively higher temperature (Orfão *et al.* 1999; Westerhof *et al*. 2012), the lower temperature during the stepwise pyrolysis generated chemicals (acids, *etc.*) other than aromatics. The low decomposition degree of cellulose at the low temperatures was the main reason for the higher yield of sugars and lower yield of furans compared with the one-step pyrolysis. The relative percentages of the acids, alcohols, nitrogen-containing compounds, and alkanes/olefins from the stepwise pyrolysis (17.06%, 4.76%, 3.92%, and 5.11%, respectively) were higher than those from the one-step pyrolysis at 500 °C (8.01%, negligible, negligible, and negligible, respectively). This was because these chemicals were mainly generated at relatively lower temperatures than 500 °C, especially the acids and nitrogen-containing compounds. For ketones/aldehydes and esters, the differences between the one-step and stepwise temperature increasing programs were not remarkable.

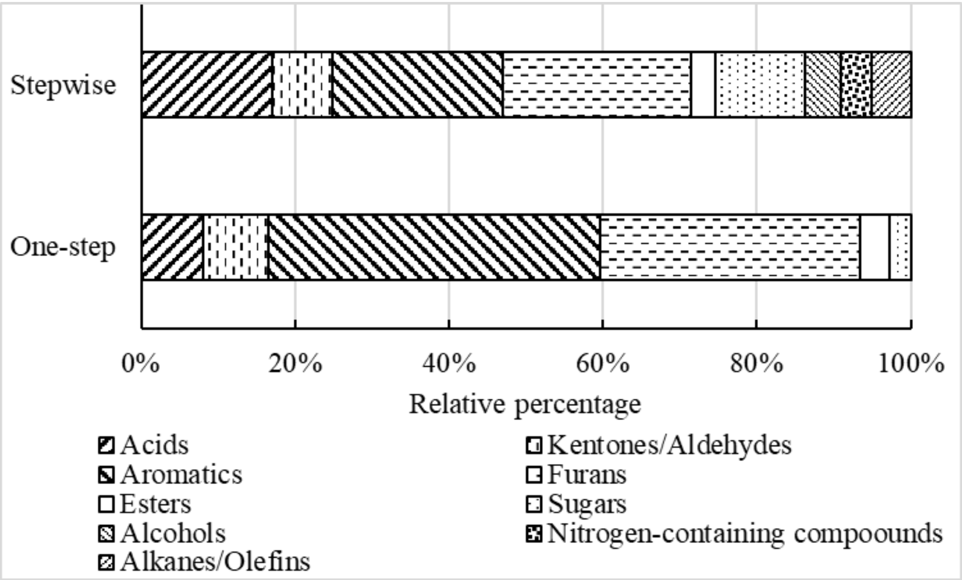

**Fig. 4.** Comparison of the chemical compounds from the one-step and stepwise pyrolysis

## Kinetic Analysis

The TG and differential thermogravimetric (DTG) curves of the FR at different heating rates are presented in Fig. 5, and the data are given in Table 3.

**Table 3.** Main TG Parameters of the FR (50 °C to 750 °C)

| Heating Rate (°C/min) | 1st Stage | 2nd Stage (Main Weight Loss Stage) | | | | 3rd Stage | Total Weight Loss (%) |
|---|---|---|---|---|---|---|---|
| | Weight Loss (%) | Temperature Region (°C) | Weight Loss (%) | Peak Temperature (°C) | Peak DTG (%/min) | Weight Loss (%) | |
| 10 | 2.16 | 120 to 375 | 45.25 | 351 | 7.25 | 14.83 | 62.24 |
| 20 | 2.90 | 120 to 383 | 44.89 | 362 | 13.66 | 14.60 | 62.39 |
| 30 | 1.34 | 120 to 390 | 46.07 | 370 | 19.96 | 14.93 | 62.34 |
| 50 | 1.68 | 120 to 403 | 47.21 | 378 | 31.03 | 14.12 | 63.01 |

The TG curve for biomass can normally be divided into three stages. The first step was moisture evaporation, which caused a slight weight loss (< 3%) under 120 °C. The second step was the main weight loss stage, which was a complex process consisting of small molecule devolatilization and decomposition of hemicellulose (shoulder peak), cellulose (main peak), and lignin (Liu 2009; Cheng *et al*. 2015a). Subsequently, the weight loss rate quickly decreased to a noticeably low level. The second stage was completed at the inflection points (375 °C to 403 °C depending on heating rate) that appeared on the DTG curves. All of the remaining TG processes occurred in the third stage, which was mainly the carbonization of the lignin residue and cross-linked sugar (Orfão *et al.* 1999).

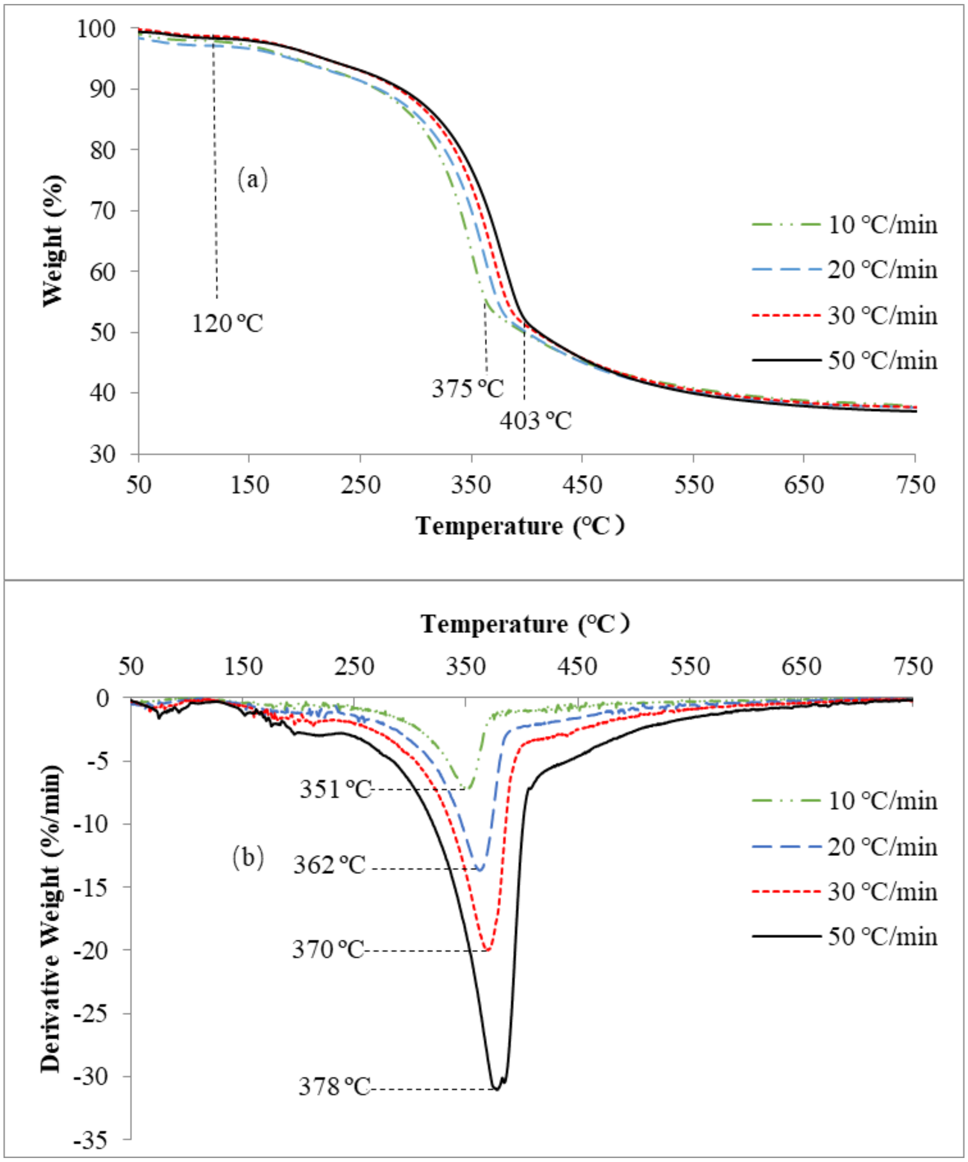

**Fig. 5.** TG (a) and DTG (b) curves of the FR at different heating rates

Compared with other biomass materials, such as bamboo, spruce, salix, miscanthus, and wheat straw (Butler *et al*. 2013; Cheng *et al*. 2015b), the shoulder peak for the hemicellulose was not found in the DTG curve of the FR because of its low hemicellulose content. According to previous reports, the peak temperature for cellulose decomposition is approximately 355 °C at a heating rate of 10 °C/min (Yang *et al*. 2007); therefore, the DTG peak of the FR at 351 °C was mainly from the decomposition of cellulose. Thus, a remarkable output of furans occurred at 350 °C during the stepwise pyrolysis of the FR, as was shown above. As the heating rate increased, the peak temperature linearly increased with increasing DTG values. The total weight loss of the FR was approximately 62% to 63%, which was much lower than that of corn cob (approximately 80%) (Worasuwannarak *et al*. 2007). This was mainly due to the fact that the high lignin content in the FR led to a high char production. Meanwhile, the ash also accounted for a relatively high proportion in the FR.

The corresponding Arrhenius plots are shown in Fig. 6. The $E_\alpha$ and coefficients of determination ($R^2$) of Arrhenius plots of the FR are summarized in Table 4. The results from the two different kinetic methods were very similar. The $E_\alpha$ of the FR increased from 178.8 kJ/mol to 212.2 kJ/mol for the FWO method, which was similar to the increase from 179.4 kJ/mol to 213.7 kJ/mol for the CR method, as $\alpha$ increased from 10% to 20%. This stage was mainly attributed to the initial decomposition of cellulose. Again, the FR was poor in hemicellulose, but rich in cellulose. The cellulose mainly decomposed before $\alpha$ increased to ~60% for the FR, and the main DTG peak of the FR was caused by cellulose decomposition. Before the main decomposition, cellulose can be partially activated in the low-temperature region, and its polymerization degree decreased (Broido and Nelson 1975; Bradbury *et al*. 1979; Tong *et al*. 2014). Meanwhile, as the TG process continued, the AAEM elements were concentrated inside the testing sample.

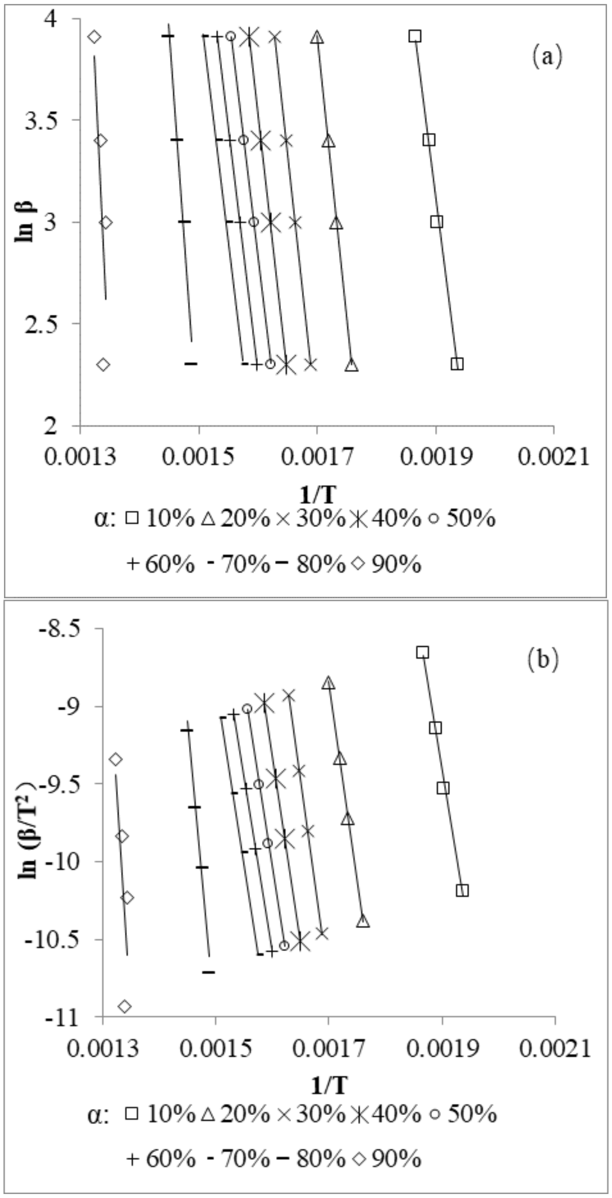

**Fig. 6.** Arrhenius plots of the FR pyrolysis using the FWO and CR methods: (a) FWO plot; (b) CR plot

The AAEM elements can exert catalytic effects (highest for cellulose, moderate for hemicellulose, and lowest for lignin) on the pyrolysis of biomass (Tan 2005). Therefore, the decreasing trend of the $E_\alpha$ for the FR as $\alpha$ increased from 20% to 60% was understandable. When $\alpha$ increased above 70%, (especially $\alpha \geq 80\%$), the $E_\alpha$ increased to an extremely high level ($\geq$ 325 kJ/mol). During the late stage of conversion, the degradation rate was noticeably reduced as the content of volatile matter decreased (Chen and Zhu 2011; Chen *et al*. 2013). The char mainly derived from lignin was rather inert, and thus it was very difficult to be activated/decomposed, even in the presence of AAEM compounds. Meanwhile, the aromatic compounds were mainly produced as the temperature increased during the stepwise pyrolysis, which also implied a higher $E_\alpha$ demand for lignin decomposition in the higher temperature region. The $R^2$ of the Arrhenius plots decreased remarkably when $\alpha$ was greater than or equal to 80%. When $\alpha$ was 90%, the $R^2$ values for the FWO and CR methods were 0.5485 and 0.5361, respectively, which indicated that the kinetic models were no longer applicable when the conversion level was very high. This change in the reaction mechanism in the high-temperature region agreed with the results of previous reports (Ozawa 1965; Song *et al*. 2015; Zhang *et al*. 2016).

**Table 4.** Kinetic Parameters of the FR Pyrolysis

| $\alpha$ (%) | FWO | | CR | |
|---|---|---|---|---|
| | $E_\alpha$ (kJ/mol) | $R^2$ | $E_\alpha$ (kJ/mol) | $R^2$ |
| 10 | 178.79 | 0.9936 | 179.35 | 0.9930 |
| 20 | 212.24 | 0.9996 | 213.66 | 0.9996 |
| 30 | 210.95 | 1 | 211.89 | 1 |
| 40 | 202.22 | 1 | 202.46 | 1 |
| 50 | 195.43 | 1 | 195.13 | 1 |
| 60 | 190.11 | 0.9999 | 189.38 | 0.9999 |
| 70 | 191.84 | 0.9994 | 191.03 | 0.9994 |
| 80 | 325.81 | 0.9749 | 331.43 | 0.9731 |
| 90 | 478.21 | 0.5485 | 490.62 | 0.5361 |

## CONCLUSIONS

1. Higher temperatures promoted the generation of aromatics, whereas lower temperatures produced nitrogen-containing compounds and acids with larger molecular weights.
2. Ketones/aldehydes, furans, esters, alcohols, and sugars all reached maximum yields at 350 °C during the stepwise pyrolysis, which was mainly attributed to the decomposition of cellulose. The aromatics and furans contents obtained from the one-step pyrolysis were much higher than those obtained from the stepwise pyrolysis. However, more acids, sugars, alcohols, nitrogen-containing compounds, and alkanes/olefins were generated during the stepwise pyrolysis.
3. The furan residue (FR) biomass featured only one DTG peak caused by cellulose decomposition. The total thermogravimetric weight loss of the FR was relatively low because of its high contents of lignin and inorganic minerals. The $E_\alpha$ of the FR

decreased as $\alpha$ increased from 20% to 60%, followed by a significant increase when $\alpha$ was more than 70%. The very high $E_\alpha$ during the late stage of conversion resulted from the carbonization process (mainly for lignin) that occurred in the high-temperature region.

## ACKNOWLEDGMENTS

This research was financially supported by the National Key R&D Program of China (2016YFE0201800) and the Priority Academic Program Development (PAPD) of Jiangsu Higher Education Institutions. The author Liang Cheng is also thankful to Zhouhong Wang for his helpful discussions. Doctor Shu Zhang would like to acknowledge the financial support from the government of Jiangsu Province.

## REFERENCES CITED

Alvira, P., Tomás-Pejó, E., Ballesteros, M., and Negro, M. J. (2010). "Pretreatment technologies for an efficient bioethanol production process based on enzymatic hydrolysis: A review," *Bioresource Technol.* 101(13), 4851-4861. DOI: 10.1016/j.biortech.2009.11.093

Azeez, A. M., Meier, D., Odermatt, J., and Willner, T. (2010). "Fast pyrolysis of African and European lignocellulosic biomasses using Py-GC/MS and fluidized bed reactor," *Energ. Fuel.* 24(3), 2078-2085. DOI: 10.1021/ef9012856

Bradbury, A. G. W., Sakai, Y., and Shafizadeh, F. (1979). "A kinetic model for pyrolysis of cellulose," *J. Appl. Polym. Sci.* 23(11), 3271-3280. DOI: 10.1002/app.1979.070231112

Broido, A., and Nelson, M. A. (1975). "Char yield on pyrolysis of cellulose," *Combust. Flame* 24, 263-268. DOI: 10.1016/0010-2180(75)90156-X

Butler, E., Devlin, G., Meier, D., and McDonnell, K. (2013). "Characterisation of spruce, salix, miscanthus and wheat straw for pyrolysis applications," *Bioresource Technol.* 131, 202-209. DOI: 10.1016/j.biortech.2012.12.013

Chen, D., and Zhu, X. (2011). "Thermal reaction mechanism of biomass and determination of activation energy II. Pyrolysis section," *Journal of Fuel Chemistry and Technology* 39(9), 670-674.

Chen, D., Zheng, Y., and Zhu, X. (2013). "In-depth investigation on the pyrolysis kinetics of raw biomass. Part I: Kinetic analysis for the drying and devolatilization stages," *Bioresource Technol.* 131, 40-46. DOI: 10.1016/j.biortech.2012.12.136

Cheng, L., Adhikari, S., Wang, Z., and Ding, Y. (2015a). "Characterization of bamboo species at different ages and bio-oil production," *J. Anal. Appl. Pyrol.* 116, 215-222. DOI: 10.1016/j.jaap.2015.09.008

Cheng, L., Adhikari, S., Wang, Z., and Ding, Y. (2015b). "Dynamic variation of fuel properties of tonkin cane (*Pseudosasa amabilis*) during maturation," *Energ. Fuel.* 29(4), 2408-2415. DOI: 10.1021/acs.energyfuels.5b00385

Cheng, L., Zhou, J., Zhang, Y., Tian, L., Ma, H., Song, J., and Zhang, Q. (2017). "Re-utilization of furfural residues and wasted mushroom inoculation bags by multi-production gasification technology," *Transactions of the Chinese Society of*

*Agricultural Engineering* 33(21), 231-236. DOI: 10.11975/j.issn.1002-6819.2017.21.028

Coats, A. W., and Redfern, J. P. (1964). "Kinetic parameters from thermogravimetric data," *Nature* 201, 68-69. DOI: 10.1038/201068a0

Cui, F. (2014). *Improvement of the Furfural Production Process*, Master's Thesis, Hebei University of Science and Technology, Shijiazhuang, China.

Demirbaş, A. (2000). "Mechanisms of liquefaction and pyrolysis reactions of biomass," *Energ. Convers. Manage.* 41(6), 633-646. DOI: 10.1016/S0196-8904(99)00130-2

Eriksson, T., Börjesson, J., and Tjerneld, F. (2002). "Mechanism of surfactant effect in enzymatic hydrolysis of lignocellulose," *Enzyme Microb. Tech.* 31(3), 353-364. DOI: 10.1016/S0141-0229(02)00134-5

Jiang, Z., Liu, Z., Fei, B., Cai, Z., Yu, Y., and Liu, X. (2012). "The pyrolysis characteristics of moso bamboo," *J. Anal. Appl. Pyrol.* 94, 48-52. DOI: 10.1016/j.jaap.2011.10.010

Liu, J. (2011). *Study on Directed Pyrolysis of Lignocellulose Biomass*, Ph.D. Thesis, Chinese Academy of Forestry, Beijing, China.

Liu, Q. (2009). *Biomass Pyrolysis Mechanism Based on the Multi-components*, Ph.D. Thesis, Zhejiang University, Hangzhou, China.

Lu, Q. (2010). *Selective Fast Pyrolysis of Biomass*, Ph.D. Thesis, University of Science and Technology of China, Hefei, China.

Lu, S. (2005). *The Analysis on the Environmental Effect of the Development of Furfural Industry in Jilin Province*, Master's Thesis, Northeast Normal University, Changchun, China.

Lv, G., and Wu, S. (2012). "Analytical pyrolysis studies of corn stalk and its three main components by TG-MS and Py-GC/MS," *J. Anal. Appl. Pyrol.* 97, 11-18. DOI: 10.1016/j.jaap.2012.04.010

Mourant, D., Wang, Z., He, M., Wang, X. S., Garcia-Perez, M., Ling, K., and Li, C.-Z. (2011). "Mallee wood fast pyrolysis: Effects of alkali and alkaline earth metallic species on the yield and composition of bio-oil," *Fuel* 90(9), 2915-2922. DOI: 10.1016/j.fuel.2011.04.033

Opfermann, J., and Kaisersberger, E. (1992). "An advantageous variant of the Ozawa-Flynn-Wall analysis," *Thermochim. Acta* 203, 167-175. DOI: 10.1016/0040-6031(92)85193-Y

Orfão, J. J. M., Antunes, F. J. A., and Figueiredo, J. L. (1999). "Pyrolysis kinetics of lignocellulosic materials—Three independent reactions model," *Fuel* 78(3), 349-358. DOI: 10.1016/S0016-2361(98)00156-2

Ozawa, T. (1965). "A new method of analyzing thermogravimetric data," *B. Chem. Soc. Jpn.* 38(11), 1881-1886. DOI: 10.1246/bcsj.38.1881

Patwardhan, P. R., Satrio, J. A., Brown, R. C., and Shanks, B. H. (2010). "Influence of inorganic salts on the primary pyrolysis products of cellulose," *Bioresource Technol.* 101(12), 4646-4655. DOI: 10.1016/j.biortech.2010.01.112

Rong, C. (2012). *Studies on Preparation of Furfural and Comprehensive Utilization of Furfural Residue*, Ph.D. Thesis, Jilin University, Changchun, China.

Slopiecka, K., Bartocci, P., and Fantozzi, F. (2012). "Thermogravimetric analysis and kinetic study of poplar wood pyrolysis," *Appl. Energ.* 97, 491-497. DOI: 10.1016/j.apenergy.2011.12.056

Song, K., Zhang, H., Wu, Q., Zhang, Z., Zhou, C., Zhang, Q., and Lei, T. (2015). "Structure and thermal properties of tar from gasification of agricultural crop residue," *J. Therm. Anal. Calorim.* 119(1), 27-35. DOI: 10.1007/s10973-014-4081-z

Sun, R. (2011). *Study on the Isolation of Lignin and the Effect of Lignin Content on the Enzymatic Hydrolysis of Furfural Residues*, Master's Thesis, Beijing Forestry University, Beijing, China.

Tan, H. (2005). *Mechanism Study of Biomass Pyrolysis*, Ph.D. Thesis, Zhejiang University, Hangzhou, China.

Tong, T. P., Ma, Z., Chen, D., and Zhang, Q. (2014). "Pyrolysis characteristics and kinetics study of bamboo holo-cellulose using TG-FTIR," *Journal of Zhejiang A&F University* 31(4), 495-501. DOI: 10.11833/j.issn.2095-0756.2014.04.001

Westerhof, R. J. M., Brilman, D. W. F., Garcia-Perez, M., Wang, Z., Oudenhoven, S. R. G., and Kersten, S. R. A. (2012). "Stepwise fast pyrolysis of pine wood," *Energ. Fuel.* 26(12), 7263-7273. DOI: 10.1021/ef301319t

Worasuwannarak, N., Sonobe, T., and Tanthapanichakoon, W. (2007). "Pyrolysis behaviors of rice straw, rice husk, and corncob by TG-MS technique," *J. Anal. Appl. Pyrol.* 78(2), 265-271. DOI: 10.1016/j.jaap.2006.08.002

Xing, Y., Bu, L. X., Wang, K., and Jiang, J. X. (2012). "Pretreatment of furfural residues with alkaline peroxide to improve cellulose hydrolysis. Characterization of isolated lignin," *Cell. Chem. Technol.* 46(3-4), 249-260.

Yang, H., Yan, R., Chen, H., Lee, D. H., and Zheng, C. (2007). "Characteristics of hemicellulose, cellulose and lignin pyrolysis," *Fuel* 86(12-13), 1781-1788. DOI: 10.1016/j.fuel.2006.12.013

Yin, Y.-L., Li, A., and Mao, L.-Y. (2011). "Progress in utilization of furfural residue utilization technology," *Modern Chemical Industry* 31(11), 22-26.

Yu, H., Li, X., Zhang, W., Sun, D., Jiang, J., and Liu, Z. (2015). "Hydrophilic pretreatment of furfural residues to improve enzymatic hydrolysis," *Cellulose* 22(3), 1675-1686. DOI: 10.1007/s10570-015-0602-6

Zeitsch, K. J. (2000). *The Chemistry and Technology of Furfural and its Many By-products*, Elsevier Publications, Amsterdam, Netherlands.

Zhang, Z., He, C., Sun, T., Zhang, Z., Song, K., Wu, Q., and Zhang, Q. (2016). "Thermo-physical properties of pretreated agricultural residues for bio-hydrogen production using thermo-gravimetric analysis," *Int. J. Hydrogen Energ.* 41(10), 5234-5242. DOI: 10.1016/j.ijhydene.2016.01.079

Zheng, T., Xing, Y., Zhou, Z., Cristhian, C., and Jiang, J. (2016). "Enhancement of bioethanol production using a blend of furfural production residue and tea-seed cake," *BioResources* 11(3), 7451-7461. DOI: 10.15376/biores.11.3.7451-7461

Article submitted: March 31, 2018; Peer review completed: April 30, 2018; Revised version received and accepted: May 21, 2018; Published: July 17, 2018.
DOI: 10.15376/biores.13.3.6678-6693